PRAMANA
—journal of
physics

Vol. 51, Nos 3 & 4
September/October 1998
pp. 387–403

CP-violating dipole form factors of the top quark and tau lepton in scalar leptoquark models

P POULOSE[a1] and SAURABH D RINDANI[a,b2]
[a] Theory Group, Physical Research Laboratory, Navrangpura, Ahmedabad 380 009, India
[b] Instituto de Física Corpuscular CSIC, Departament de Física Teòrica, Universitat de València, 46100 Burjassot (València), Spain
[1] Present address: Theory Group, Tata Institute of Fundamental Research, Homi Bhabha Road, Colaba, Mumbai 400 005; email address: poulose@theory.tifr.res.in
[2] E mail address: saurabh@prl.ernet.in

MS received 12 February 1998; revised 4 June 1998

Abstract. We calculate the CP-violating electric and weak dipole form factors of the top quark and the tau lepton in models with scalar leptoquarks coupling only to the third generation of quarks and leptons. We obtain numerical values of the real and imaginary parts of these form factors at various energies for different values of leptoquark masses and couplings. The existing limits on the tau electric and weak dipole form factors allow us to put a limit on the masses and couplings of such leptoquarks and therefore on the top electric and weak dipole form factors. We also discuss constraints on the form factors coming from indirect limits on leptoquark masses and couplings deduced from LEP results on Z properties.

Keywords. CP violation; scalar leptoquarks; dipole moments; top quark; tau lepton.

PACS Nos 11.30; 13.40; 14.60; 14.65

1. Introduction

The standard model (SM) of electroweak interactions predicts that CP violation outside the K- and B-meson systems would be unobservably small. Thus, if any CP violation is observed in the future outside of these systems, it would be a signal of new physics. In particular, the observation of electric dipole moments of elementary particles would signal new mechanisms of CP violation lying beyond SM, since SM predicts unobservably small electric dipole moments. Likewise, their generalization to Z couplings (the so-called weak dipole moments), as well as to couplings at nonzero momentum transfers, viz., dipole form factors (DFF), would also serve as signals for CP violation beyond SM.

Recent experiments at the Large Electron Positron Collider (LEP) at CERN have established an upper bound on the weak dipole form factor of the tau lepton at the Z peak, by looking for CP-violating momentum correlations [1, 2]. The latest result is from the OPAL collaboration [2], who have obtained the limits

$$\mathrm{Re}\, d_\tau^Z < 5.6 \times 10^{-18}\, e\,\mathrm{cm},$$
$$\mathrm{Im}\, d_\tau^Z < 1.5 \times 10^{-17}\, e\,\mathrm{cm}.$$

It is expected that better limits would be obtained in future experiments using longitudinally polarized electrons [3]. For example, it was shown that using certain CP-odd vector correlations, it would be possible to measure an EDFF of τ of the order of $10^{-19}\, e$ cm [3].

Estimates have also been made of the sensitivity to which various experiments at e^+e^- [4] as well as hadron colliders [5] might be able to measure top electric and weak dipole form factors.

Most models seem to predict values of electric dipole form factors (EDFF) and weak dipole form factors (WDFF) an order of magnitude below the observable level in the next generation of planned experiments. In this situation, it is a worthwhile pursuit to look at other models which might predict large DFF's which could be tested in the near future.

In this paper we consider the possibility that models with relatively light scalars with complex couplings to a third-generation lepton quark pair can give rise to EDFF and WDFF of third generation fermions, viz., the top quark and the tau lepton, at a significant level. This possibility for the tau lepton has been considered recently by Mahanta [6] and Bernreuther *et al* [7]. While we confirm some results for tau of [6] and [7], we also obtain new results for the CP-violating form factors of the top quark, and treat the tau and top cases in a concerted manner. We have also studied the implications of the existing experimental bounds from LEP on the weak dipole form factor of τ at the Z resonance, and on the masses and couplings of leptoquarks from loop effects contributing to the Z partial widths.

A large number of extensions of SM predict the existence of colour triplet particles carrying simultaneously lepton and baryon number, called leptoquarks. These models include grand unified theories, technicolour models, superstring inspired models and composite models. Without reference to specific models, the masses and couplings of leptoquarks can be constrained using low-energy experiments. These experiments test predictions of leptoquark interactions for atomic parity violation, meson decay, flavour-changing neutral currents and meson-antimeson mixing.

There have been several direct searches for leptoquarks at high energy accelerators. At LEP, a lower bound of 45–73 GeV for the mass of leptoquarks was put [8]. The limit coming from $p\bar{p}$ colliders is 175 GeV from D0 [9] and 131–133 GeV from CDF [10] on the mass of a scalar leptoquark decaying into an electron-jet pair. On the mass of the third generation scalar leptoquark decaying into $b\tau$, CDF has given a bound of 99 GeV [10] and a bound of 94 GeV was obtained by D0 for such a leptoquark decaying into $b\nu_\tau$ [9]. The excess of large-Q^2 events reported in e^+p collisions at HERA [11] have been interpreted as due to leptoquark production [12], the mass of the leptoquark being around 200 GeV. The earlier limit coming from HERA is dependent on the leptoquark type and couplings, and the lower bound is between 92 and 184 GeV [13]. Bounds possible at future pp, ep, e^+e^-, $e\gamma$ and $\gamma\gamma$ experiments have been a topic of serious study.

Indirect bounds on masses and couplings can be obtained from the results of low-energy experiments [14]. However, these constraints are strong only for leptoquarks that couple to quarks and leptons of the first and second generations.

While there are strong constraints on masses of leptoquarks which also couple to pairs of quarks, thus violating baryon number as well as lepton number, the constraints on the

couplings and masses of leptoquarks which do not couple to two quarks are weaker. Moreover, these constraints are strongest for the first and second generations, and considerably weaker for leptoquarks coupling only to the third generation of quarks and leptons.

Strong constraints on leptoquarks which couple to leptons and quarks of the third generation have been obtained from their contributions to the radiative corrections to Z properties [15, 16, 17]. The authors of [15] have studied vertex corrections to the leptonic partial widths of the Z induced by leptoquark loops and obtained stringent constraints on leptoquark masses and couplings. The authors of [16, 17] performed a global fit to the LEP data including contributions from a scalar leptoquark loop. They also arrive at stringent constraints on leptoquark masses and couplings.

Earlier work on CP violation in leptoquark models can be found in [18, 19].

In this paper, we calculate the EDFF and WDFF for the third generation fermions, viz., the top quark and the tau lepton, in scalar leptoquark models within the context of an $SU(2)_L \times U(1) \times SU(3)_c$ gauge theory, where the leptoquarks couple to only the third generation fermions. We then use the indirect limits obtained from LEP on the masses and couplings of the leptoquark to investigate the possible values of the EDFF and WDFF in these models that are consistent with these limits.

Briefly, our results are as follows. The present experimental limits on τ EDFF and WDFF do not put stringent constraints on masses and couplings of leptoquarks. Consequently, these results are consistent with a top EDFF of the order of $10^{-19}e$cm, and a top WDFF of the order of $10^{-20}e$ cm. The indirect LEP limits, however, constrain these form factors to be at least three orders of magnitude lower. They also give limits on tau form factors about two orders of magnitude lower than the direct experimental limits.

We describe in the next section couplings of scalar leptoquarks with various transformation properties under $SU(2)_L \times U(1) \times SU(3)_c$. In § 3, we give expressions for the imaginary parts of the EDFFs and WDFFs of τ and t arising from these leptoquark couplings, and write dispersion relations for obtaining the corresponding real parts. In § 4 we present numerical results and the last section (§ 5) contains our conclusions.

2. Scalar leptoquark couplings

We will describe in this section leptoquark couplings in an $SU(2)_L \times U(1) \times SU(3)_c$ gauge theory, assuming that baryon-number violating couplings to diquarks are somehow forbidden, as required by strong bounds on proton-decay searches. In that case, the only possible leptoquark representations which could have couplings to the standard-model representations of quarks and leptons are as shown in table 1, together with their quantum numbers [20].

The most general Lagrangian containing all possible forms of couplings of scalar leptoquarks to a lepton and quark pair is given by

$$\mathcal{L}_{\text{eff}} = \mathcal{L}_{F=2} + \mathcal{L}_{F=0}, \tag{1}$$

where

$$\mathcal{L}_{F=0} = h_{2L}\overline{u_R}R_2^T i\tau_2 l_L + h_{2R}\overline{q_L}e_R R_2 + \tilde{h}_{2L}\overline{d_R}\tilde{R}_2^T i\tau_2 l_L + h.c., \tag{2}$$

Table 1. $SU(2)_L$, $U(1)$, $SU(3)_c$ and electric charge assignments of the various leptoquarks.

	$SU(2)_L$	$U(1)$	$SU(3)_c$	Q
S_1	1	$\frac{1}{3}$	3^*	$\frac{1}{3}$
$\tilde{S}_1$	1	$\frac{4}{3}$	3^*	$\frac{4}{3}$
S_3	3	$\frac{1}{3}$	3^*	$\frac{4}{3}, \frac{1}{3}, \frac{-2}{3}$
R_2	2	$\frac{7}{6}$	3	$\frac{5}{3}, \frac{2}{3}$
$\tilde{R}_2$	2	$\frac{1}{6}$	3	$\frac{2}{3}, \frac{-1}{3}$

and

$$\mathcal{L}_{F=2} = (g_{1L}\overline{q_R^c} i\tau_2 l_L + g_{1R}\overline{u_L^c} e_R) S_1 + \tilde{g}_{1R}\overline{d_L^c} e_R \tilde{S}_1 + g_{3L}\overline{q_R^c} i\tau_2 \vec{\tau} l_L \cdot \vec{S}_3 + h.c.. \quad (3)$$

The two pieces correspond to the fermion number $F = 0$ for the leptoquarks R_2 and $\tilde{R}_2$, and $F = -2$ for S_1, $\tilde{S}_1$ and S_3. Colour indices are suppressed in writing eqs (2) and (3).

Of the various couplings in eqs (2) and (3), those of $\tilde{S}_1$ and $\tilde{R}_2$ do not contribute to τ and t DFFs in the limit of massless neutrinos and b quark, and so we will not consider these. Moreover, as we shall see, for a DFF to be nonzero, both left- and right-handed couplings are required to be present. Thus, we find that since S_3 has only left-handed coupling to leptons, it does not contribute to the DFFs. We will therefore not consider S_3 either.

The low-energy constraints arising from decays of pseudoscalar mesons are very stringent, unless the leptoquark couplings to the light quarks are chiral. Hence many authors assume couplings to be either left-handed or right-handed. However, we are going to consider only the third generation leptoquarks on whose couplings there are no strong limits from meson decays. So we need not assume their couplings to be chiral. More importantly, we need both left- and right-handed couplings to be present for the EDFF and WDFF to be nonzero. If, however, the third generation leptoquarks mix substantially with those of the first and second generations, the low-energy constraints would apply more or less unchanged. We will therefore assume mixing to be absent.

While only one of the components of each leptoquark multiplets would contribute to the form factors we calculate, it is important to note that the constraints we will use on the leptoquark couplings and masses were derived assuming that leptoquarks within a multiplet are degenerate [15, 16, 17]. Though strict degeneracy is not required, these authors were motivated to make this assumption to avoid conflict with the ρ parameter, which is constrained to be close to 1 by LEP experiments [21]. These constraints were also derived under the assumption of chiral couplings for leptoquarks. However, in the presence of both left-handed and right-handed couplings, the constraints are expected to be somewhat more stringent. We have, however, chosen the constraints on left-handed couplings for our analysis, since these are more stringent.

The couplings of leptoquarks to a single γ or Z is given by

$$\mathcal{L}_{\gamma,Z} = -ie \sum_i \phi_i^\dagger \overleftrightarrow{\partial_\mu} \phi_i \left[Q_i A^\mu - \frac{T_{3L} - Q_i s_W^2}{s_W c_W} Z^\mu \right], \quad (4)$$

where ϕ_i are the various scalar fields, T_{3i} and Q_i are the respective values of the third component of weak isospin and electric charge, and $c_W = \cos\theta_W$, $s_W = \sin\theta_W$, θ_W being the weak mixing angle.

We use the couplings written down in eqs (2), (3) and (4) to obtain expressions for the EDFF and WDFF of τ and t at the one-loop level in the next section.

3. Electric and weak dipole form factors

Using the leptoquark couplings described in the last section we shall look at the one-loop corrections to the $t\bar{t}(\gamma, Z)$ vertices. We use Cutkosky rules [22] to calculate the imaginary part of the DFF and from this the real part is obtained using a dispersion relation. This method has certain advantages over the standard method of calculating loop contributions, particularly when the quantity of interest, in our case the DFF, is not present at tree level. In such a case, the loop contribution has to be finite in a renormalizable theory, and this guarantees that the dispersion integral is convergent. Thus one does not have to worry about cancellation of divergences between sets of diagrams. Moreover, when one calculates the imaginary parts using the Cutkosky rules, the intermediate states contain only physical, on-shell particles, thus doing away with the need for unphysical scalars, ghosts, etc. Thus the number of diagrams to be handled is less as compared to the standard method, as also the convergence of integrals is ensured. In addition, dispersion integrals, when evaluated numerically, have better convergence as compared to, for example the popular Passarino-Veltman method because of better handling of particle thresholds.

3.1 *EDFF and WDFF of the top quark*

At one-loop level the diagrams giving rise to the correction to the $t\bar{t}(\gamma, Z)$ coupling due to the leptoquark are given in figure 1. We use the symbol ϕ for the generic leptoquark.

The lepton could be ν_τ instead of τ interacting with a leptoquark of different T_3 and Q values. However, as we shall see, the contribution to the CP-violating DFFs turns out to be proportional to the mass of the virtual lepton because of chirality flip in scalar couplings. In the limit of small ν_τ mass, only the τ contribution is present.

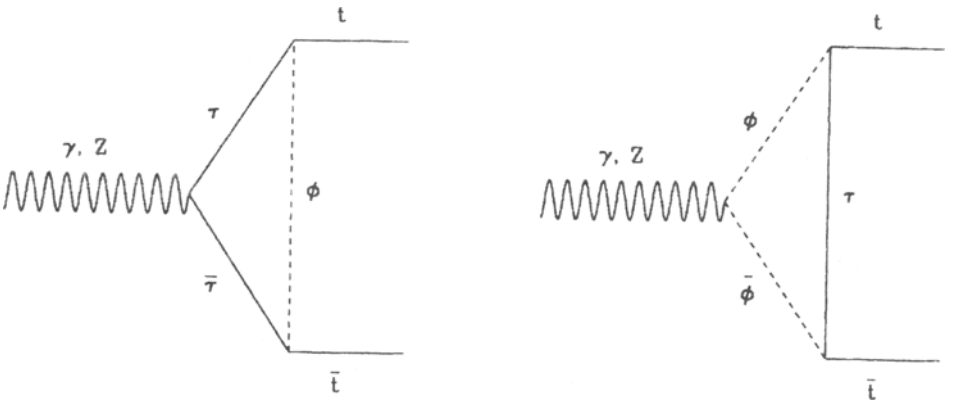

Figure 1. Feynman diagrams corresponding to one-loop correction to the $t\bar{t}(\gamma, Z)$ vertex in the presence of a third generation leptoquark.

We use Cutkosky rules to calculate the absorptive part of the process. This means considering intermediate particles to be on shell and hence the conditions on the γ/Z boson momentum q for diagram in figure 1 are $q^2 > 4m_\tau^2$ and $q^2 > 4m_\phi^2$ in case of τ pair production and leptoquark pair production respectively, where m_ϕ is the leptoquark mass. We calculate the vertex contribution coming from these two diagrams.

Using the couplings given in eqs (2) and (3) we obtain the imaginary part of the top quark EDFF and WDFF as

$$\begin{aligned}
\mathrm{Im}d_t^\gamma(s) &= \frac{eg_\phi^2}{4\pi s} m_\tau \mathrm{Im}(a^* b)\{-F_1^t(s) + QF_2^t(s)\},\\
\mathrm{Im}d_t^Z(s) &= \frac{eg_\phi^2}{4\pi s \sin\theta_W \cos\theta_W} m_\tau \mathrm{Im}(a^* b)\\
&\quad \times \{\tfrac{1}{2}(-\tfrac{1}{2} + 2\sin^2\theta_W)F_1^t(s) + (T_3 - Q\sin^2\theta_W)F_2^t(s)\},
\end{aligned} \tag{5}$$

where

$$\begin{aligned}
F_1^t(s) = \frac{1}{\beta_t^2}\Bigg\{&\beta_\tau + \frac{1}{s\beta_t}(m_t^2 + m_\phi^2 - m_\tau^2)\\
&\times \ln\left[\frac{2(m_t^2 + m_\tau^2 - m_\phi^2) - s(1 - \beta_t\beta_\tau)}{2(m_t^2 + m_\tau^2 - m_\phi^2) - s(1 + \beta_t\beta_\tau)}\right]\Bigg\}\theta(s - 4m_t^2),
\end{aligned} \tag{6}$$

and

$$\begin{aligned}
F_2^t(s) = \frac{1}{\beta_t^2}\Bigg\{&\beta_\phi - \frac{1}{s\beta_t}\left(m_t^2 + m_\phi^2 - m_\tau^2 - \frac{s}{2}\right)\\
&\times \ln\left[\frac{2(m_t^2 - m_\tau^2 + m_\phi^2) - s(1 - \beta_t\beta_\phi)}{2(m_t^2 - m_\tau^2 + m_\phi^2) - s(1 + \beta_t\beta_\phi)}\right]\Bigg\}\theta(s - 4m_\phi^2).
\end{aligned} \tag{7}$$

In the above equation, T_3 and Q refer respectively to the third component of isospin and charge of the leptoquark ϕ, g_ϕ is the absolute value of the coupling constant, assuming $|g_L| = |g_R|$ (and $|h_{2L}| = |h_{2R}|$) occurring in eqs (2) and (3), and a and b are phase factors of the corresponding vector and axial vector couplings. β_t, β_τ and β_ϕ refer to the velocities of t, τ and ϕ,

$$\beta_{t,\tau,\phi} = \sqrt{1 - \frac{4m_{t,\tau,\phi}^2}{s}}. \tag{8}$$

The expression in eq. (6) is valid for $s > 4m_t^2$. $F_1^t(s)$ for $2m_\tau < \sqrt{s} < 2m_t$ is given by the analytic continuation of eq. (6):

$$\begin{aligned}
F_1^t(s) = \frac{1}{\beta_t^2}\Bigg\{&\beta_\tau + \frac{2}{s\sqrt{-\beta_t^2}}(m_t^2 + m_\phi^2 - m_\tau^2)\\
&\times \tan^{-1}\left[\frac{\sqrt{-\beta_t^2}\beta_\tau s}{2(m_t^2 + m_\tau^2 - m_\phi^2) - s}\right]\Bigg\}\theta(s - 4m_\tau^2)\theta(4m_t^2 - s).
\end{aligned} \tag{9}$$

The real parts of the form factors are obtained using an unsubtracted dispersion relation

$$\mathrm{Re}\, d_t^{\gamma,Z}(s) = \frac{\mathrm{P}}{\pi}\int_{4m_\tau^2}^{\infty} \frac{\mathrm{Im} d_t^{\gamma,Z}(s')}{s'-s}\,\mathrm{d}s', \tag{10}$$

where P denotes the principal part of the integral.

It can be seen that the dispersion integrals are convergent and do not need any subtraction. This is to be expected since the dipole form factors, which correspond to dimension 5 operators, should be finite in a renormalizable theory.

3.2 *EDFF and WDFF of the τ lepton*

The EDFF and WDFF of the tau lepton also arise in the same leptoquark theory from diagrams exactly analogous to the ones in figure 1, with the roles of t and τ interchanged. Proceeding exactly as in the previous section, we obtain expressions for the imaginary parts of the tau lepton EDFF and WDFF, neglecting the b mass.

$$\begin{aligned}
\mathrm{Im}\, d_\tau^{\gamma}(s) &= \frac{3eg_\phi^2}{4\pi s} m_t \mathrm{Im}(a^* b)\left\{\frac{2}{3}F_1^\tau(s) - QF_2^\tau(s)\right\},\\
\mathrm{Im}\, d_\tau^{Z}(s) &= \frac{3eg_\phi^2}{4\pi s \sin\theta_W \cos\theta_W} m_t \mathrm{Im}(a^* b)\\
&\quad\times\left\{\frac{1}{2}\left(\frac{1}{2}-\frac{4}{3}\sin^2\theta_W\right)F_1^\tau(s) - (T_3 - Q\sin^2\theta_W)F_2^\tau(s)\right\},
\end{aligned} \tag{11}$$

where

$$\begin{aligned}
F_1^\tau(s) =& \frac{1}{\beta_\tau^2}\left\{\beta_t + \frac{1}{s\beta_\tau}(m_\tau^2 + m_\phi^2 - m_t^2)\right.\\
&\left.\times \ln\left[\frac{2(m_\tau^2 + m_t^2 - m_\phi^2) - s(1-\beta_t\beta_\tau)}{2(m_\tau^2 + m_t^2 - m_\phi^2) - s(1+\beta_t\beta_\tau)}\right]\right\}\theta(s-4m_t^2),
\end{aligned} \tag{12}$$

and

$$\begin{aligned}
F_2^\tau(s) =& \frac{1}{\beta_\tau^2}\left\{\beta_\phi - \frac{1}{s\beta_\tau}\left(m_\tau^2 + m_\phi^2 - m_t^2 - \frac{s}{2}\right)\right.\\
&\left.\times \ln\left[\frac{2(m_\tau^2 - m_t^2 + m_\phi^2) - s(1-\beta_\tau\beta_\phi)}{2(m_\tau^2 - m_t^2 + m_\phi^2) - s(1+\beta_\tau\beta_\phi)}\right]\right\}\theta(s-4m_\phi^2).
\end{aligned} \tag{13}$$

Since both m_t and m_ϕ are larger than m_τ, there is no domain where an analytic continuation is needed.

As before, the real parts of the form factors are given by the unsubtracted dispersion relations:

$$\mathrm{Re}\, d_\tau^{\gamma,Z}(s) = \frac{\mathrm{P}}{\pi}\int_{4m_\tau^2}^{\infty} \frac{\mathrm{Im}\, d_\tau^{\gamma,Z}(s')}{s'-s}\,\mathrm{d}s'. \tag{14}$$

In the next section we will evaluate the real and imaginary parts of the t and τ form factors numerically for different choices of masses and couplings of the leptoquarks.

Using the experimental limits on the tau lepton DFFs we obtain bounds on the masses and couplings of the leptoquarks.

4. Numerical results

We use here the expressions of the previous section to get numerical values for the various form factors. While we have analytic expressions for the imaginary parts, the real parts, given by the dispersion integrals, have been evaluated by numerical integration.

To investigate how large the form factors can be, consistent with LEP constraints, we have plotted the τ and t form factors as functions of $\sqrt{s}$. We have chosen $m_t = 180\,\text{GeV}$

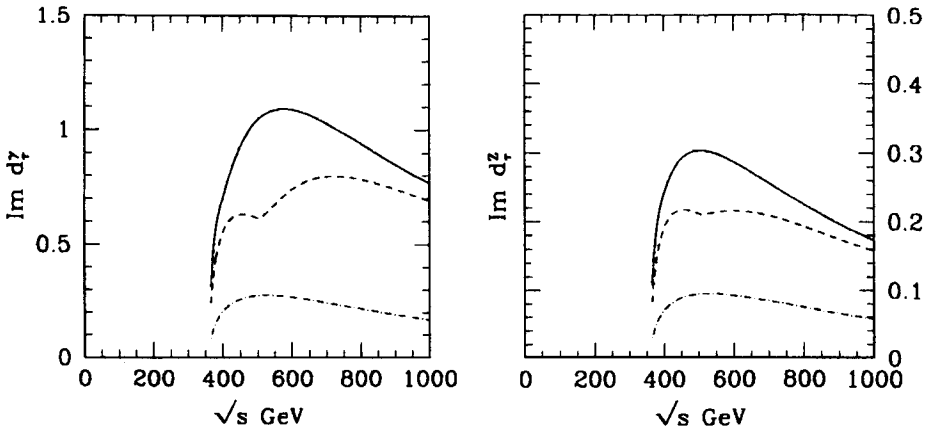

Figure 2. Imaginary parts of the electric (figure on the left) and weak (figure on the right) dipole form factors of τ in units of $10^{-18}\,e$ cm as functions of c.m. energy $\sqrt{s}$ for the model with leptoquark R_2. Solid, dashed and dash-dotted lines correspond to leptoquark masses of 200, 250 and 500 GeV respectively. g_ϕ is chosen to be 1.

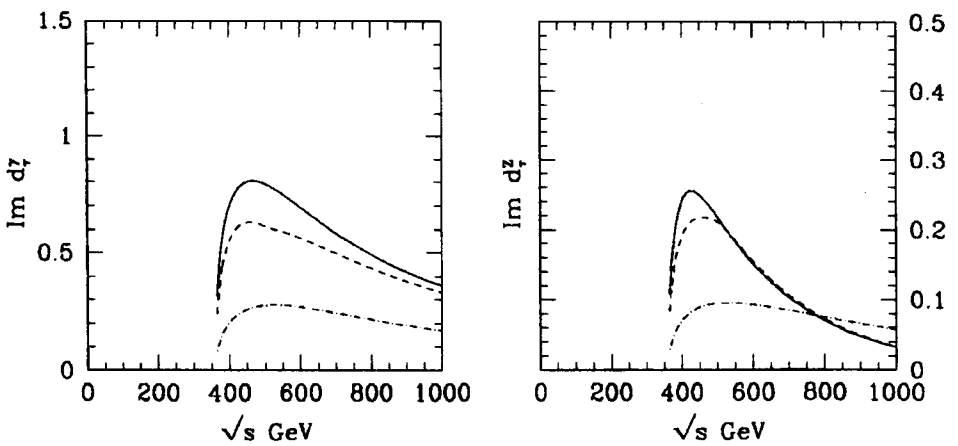

Figure 3. Imaginary parts of the electric (figure on the left) and weak (figure on the right) dipole form factors of τ in units of $10^{-18}\,e$ cm as functions of c.m. energy $\sqrt{s}$ for the model with leptoquark S_1. Solid, dashed and dash-dotted lines correspond to leptoquark masses of 200, 250 and 500 GeV respectively. g_ϕ is chosen to be 1.

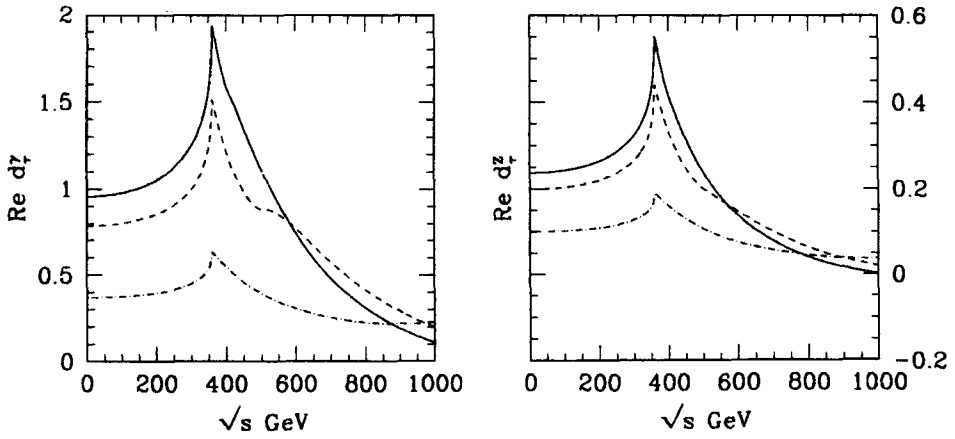

Figure 4. Real parts of the electric (figure on the left) and weak (figure on the right) dipole form factors of τ in units of $10^{-18}\,e$ cm as functions of c.m. energy $\sqrt{s}$ for the model with leptoquark R_2. Solid, dashed and dash-dotted lines correspond to leptoquark masses of 200, 250 and 500 GeV respectively. g_ϕ is chosen to be 1.

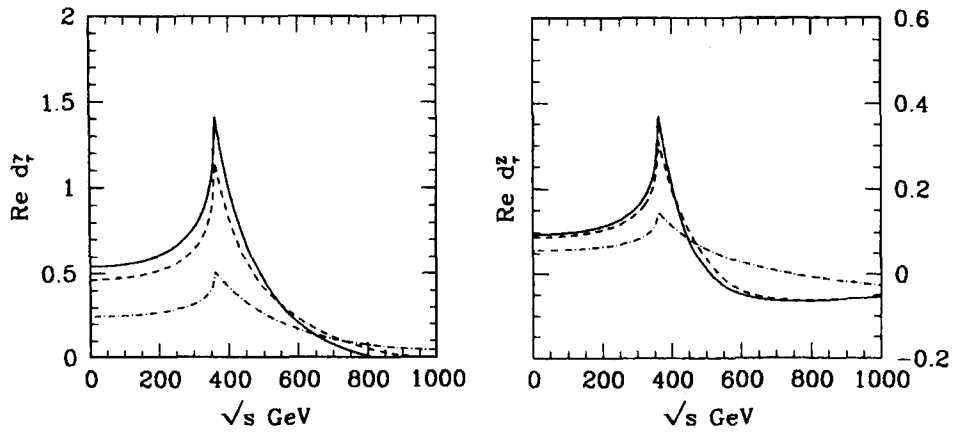

Figure 5. Real parts of the electric (figure on the left) and weak (figure on the right) dipole form factors of τ in units of $10^{-18}\,e$ cm as functions of c.m. energy $\sqrt{s}$ for the model with leptoquark S_1. Solid, dashed and dash-dotted lines correspond to leptoquark masses of 200, 250 and 500 GeV respectively. g_ϕ is chosen to be 1.

and a maximal value $\mathrm{Im}(a^*b) = 1/2$. We have considered three different leptoquark masses, viz., 200, 250 and 500 GeV. g_ϕ is chosen to be 1. In all cases dipole form factors are smaller for higher leptoquark masses up to around c.m. energy of 500 GeV. This dependence on leptoquark masses for a fixed $\sqrt{s}$ is as should be expected. For the imaginary parts of the form factors, it is only on-shell intermediate states which contribute. Hence, for given $\sqrt{s}$, heavier particles would contribute less – either because of phase space suppression, or because of propagator effects. For fixed $\sqrt{s}$, the mass dependence of even the real parts follows that of the imaginary part which comes in the numerator of the dispersion integral. At higher energies dependence on the mass becomes

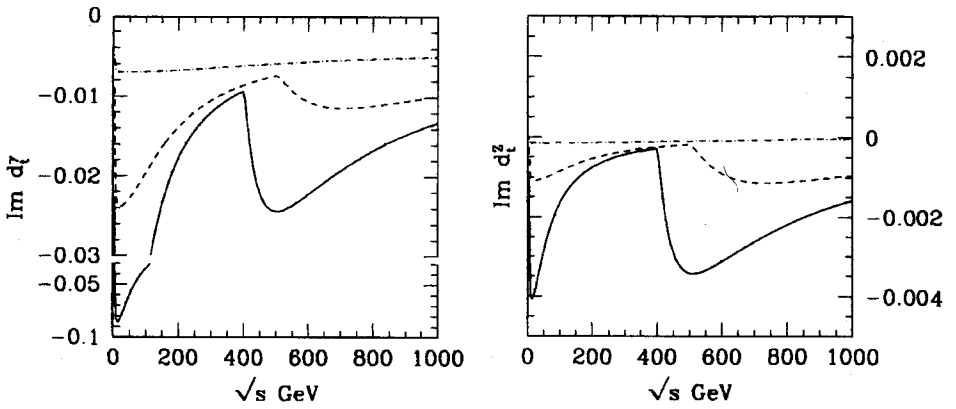

Figure 6. Imaginary parts of the electric (figure on the left) and weak (figure on the right) dipole form factors of the top quark in units of $10^{-18}\,e$ cm as functions of c.m. energy $\sqrt{s}$ for the model with leptoquark R_2. Solid, dashed and dash-dotted lines correspond to leptoquark masses of 200, 250 and 500 GeV respectively. g_ϕ is chosen to be 1.

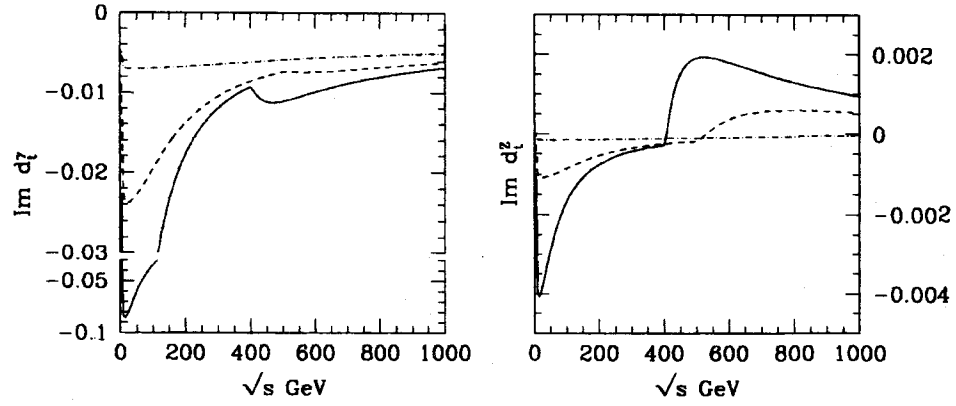

Figure 7. Imaginary parts of the electric (figure on the left) and weak (figure on the right) dipole form factors of the top quark in units of $10^{-18}\,e$ cm as functions of c.m. energy $\sqrt{s}$ for the model with leptoquark S_1. Solid, dashed and dash-dotted lines correspond to leptoquark masses of 200, 250 and 500 GeV respectively. g_ϕ is chosen to be 1.

weaker than that at lower energies. This can be understood from the fact that there is no longer phase-space suppression, and the mass-dependence of propagators is weak.

Among the leptoquarks belonging to the two representations considered, R_2 (see table 1 for quantum numbers) gives larger form factors than S_1.

Figures 2 and 3 show the dependence of the imaginary parts of the τ EDFF and WDFF on the c.m. energy. Similarly, figures 4 and 5 show the dependence of the real parts. Since the top quark mass is assumed to be 180 GeV, there is a peak at 360 GeV. A similar behaviour is seen at the leptoquark threshold. However, in the case of the WDFF for both R_2 and S_1 leptoquarks, and in the case of EDFF for the S_1 leptoquark, the leptoquark

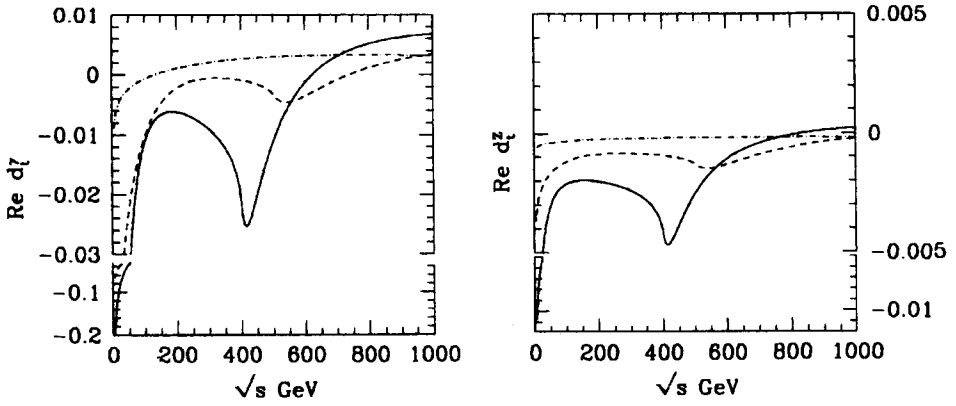

Figure 8. Real parts of the electric (figure on the left) and weak (figure on the right) dipole form factors of the top quark in units of 10^{-18} e cm as functions of c.m. energy $\sqrt{s}$ for the model with leptoquark R_2. Solid, dashed and dash-dotted lines correspond to leptoquark masses of 200, 250 and 500 GeV respectively. g_ϕ is chosen to be 1.

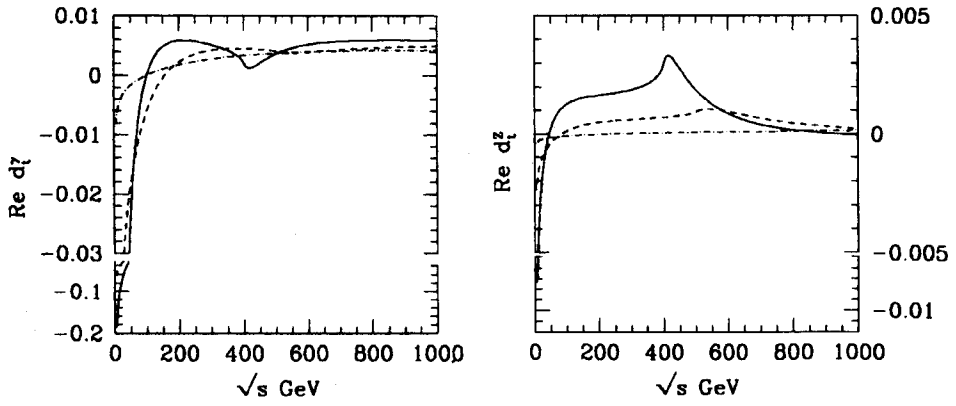

Figure 9. Real parts of the electric (figure on the left) and weak (figure on the right) dipole form factors of the top quark in units of 10^{-18} e cm as functions of c.m. energy $\sqrt{s}$ for the model with leptoquark S_1. Solid, dashed and dash-dotted lines correspond to leptoquark masses of 200, 250 and 500 GeV respectively. g_ϕ is chosen to be 1.

threshold effect is not so prominent because the relevant leptoquark charge is numerically small.

Figures 6 and 7 show the variation of the imaginary part of the t DFFs with c.m. energy, and figures 8 and 9 show the corresponding curves for the real parts [23]. The behaviour is similar to that in the tau case with peaks at τ and leptoquark resonances. In the case of the top quark form factors, it is interesting to observe the difference in signs, especially of the WDFF, between the R_2 and S_1 leptoquark models.

It is seen from the curves that in general, the R_2 model gives larger values of the form factors compared to the S_1 model. We therefore concentrate on the R_2 model in what follows.

At a fixed c.m. energy the form factors are functions of two parameters – the mass and the coupling of the leptoquark considered. From an assumed value of the form factor it is

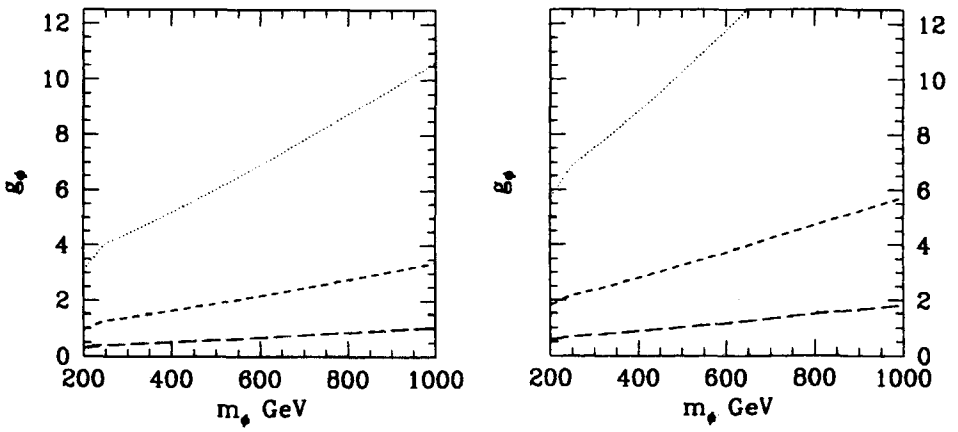

Figure 10. Contours in the mass-coupling plane for different values of imaginary parts of EDFF (left) and WDFF (right) of τ for the R_2 model. Dotted, dashed and long dashed lines correspond to DFF values of 10^{-17}, 10^{-18} and 10^{-19} e cm, respectively, A c.m. energy of 500 GeV is assumed.

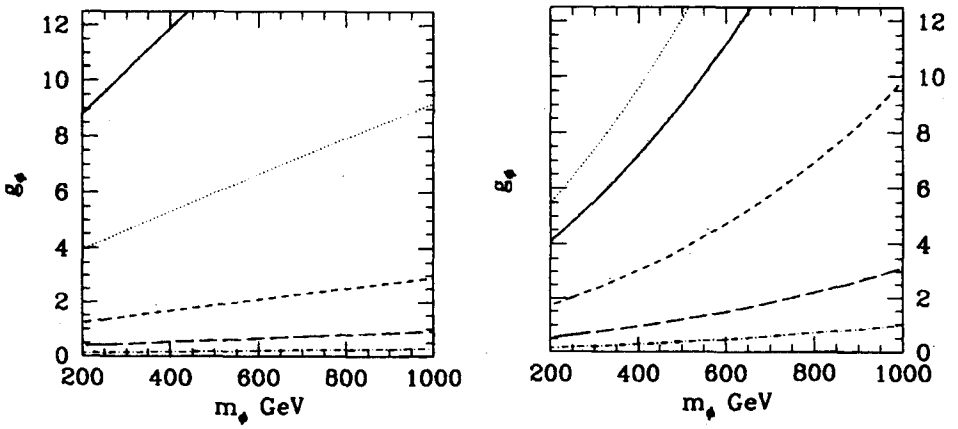

Figure 11. Contours in the mass-coupling plane for different values of the real parts of EDFF (left) and WDFF (right) of τ for the R_2 model. Types of lines and corresponding DFF values are the same as those in figure 10 except that the dash-dotted line corresponds to a DFF value of 10^{-20} e cm, and the solid curve corresponds to the experimental bounds on the dipole moments, which are $d_\tau^\gamma = 5 \times 10^{-17}$ e cm, $\mathrm{Re}\, d_\tau^Z = 5.6 \times 10^{-18}$ e cm. EDFF values are at a c.m. energy of 4 GeV while WDFF values are at 91.18 GeV. Top-quark mass is taken to be 180 GeV in all cases.

possible to get contours in the plane of the mass and coupling constant of the leptoquark. Contours in the mass-coupling plane for the doublet R_2 leptoquark model are given for different values of tau lepton DFF's in figures 10 and 11. The validity of perturbation theory allows values of coupling $g_\phi < 4\pi$. In the case of the tau lepton we have considered the present experimental limits on the dipole moments.

Figure 11 shows the allowed region in the $m_\phi - g_\phi$ plane which lies below the solid line if we consider the present experimental limit on the tau electric dipole moment. No

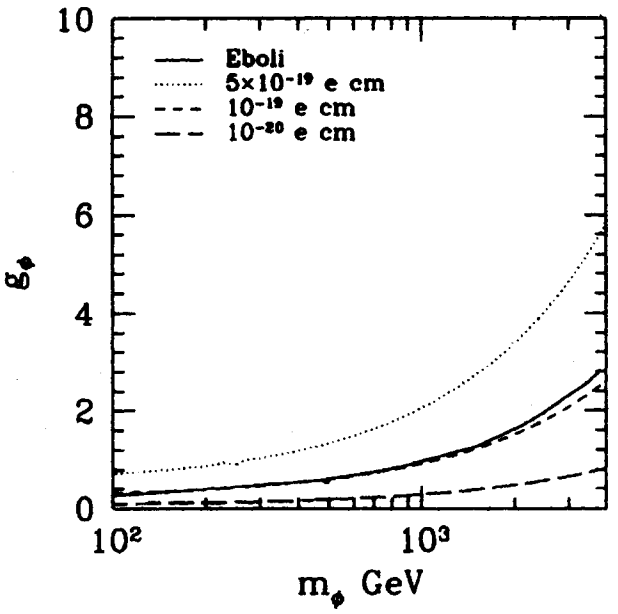

Figure 12. Contours in the mass-coupling plane for the R_2 leptoquark model. The solid line represents the limits from the one-loop calculation by Éboli [17] while the other curves correspond to different values of the real part of the tau EDFF. Top-quark mass of 175 GeV is assumed. The c.m. energy used is 500 GeV.

value of m_ϕ or g_ϕ is completely excluded. However, it is possible that future experiments may give more stringent limits on dipole form factors which may put upper bounds on the coupling or lower bounds on the mass.

As mentioned before, LEP results on Z partial widths have been used to obtain constraints on masses and couplings for third-generation leptoquarks [15–17]. We have chosen Éboli's [17] limits to compare with the constraints we get from the dipole form factors. The other limits would give similar results. Figure 12 shows contours for different values of the real part of the electric dipole form factor of τ along with the limit obtained by Éboli [17] in the $m_\phi - g_\phi$ plane. To accommodate their limits we have to restrict the electric dipole form factors of τ to be smaller than about $10^{-19}\,e$ cm. A similar analysis shows that the weak dipole form factors must be smaller than about $10^{-20}\,e$ cm.

The best limit on m_ϕ and g_ϕ obtainable from the experimental limits on form factors is that from the real part of the weak dipole moment of the tau lepton, and we use that limit in what follows.

In the case of top quark there are no experimental limits. From the constraints obtained on the mass and the coupling from the experimental bound on the real part of the tau WDFF, figures 13 and 14 show that the top quark can have values for the imaginary part of the EDFF as high as $10^{-19}\,e$ cm except for a small mass range ($\sim$ 250–300 GeV). The imaginary part of the weak dipole form factor of the top quark is allowed to be almost as high as $10^{-20}\,e$ cm. We get more or less the same limits for the real part of both the electric and the weak dipole form factors.

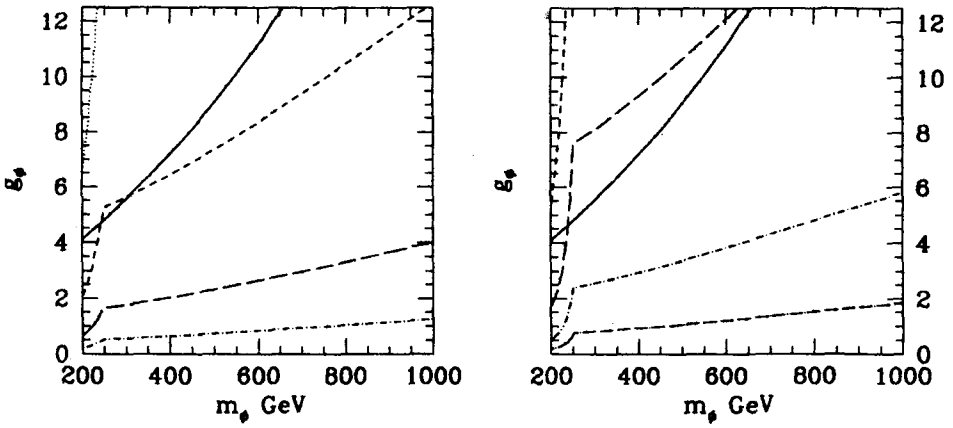

Figure 13. Contours in the mass-coupling plane for different values of imaginary parts of the top EDFF (the figure on the left) and WDFF (the figure on the right). Dotted, dashed, long dashed, dash-dotted and long dash-dotted lines correspond to DFF values of $10^{-18}, 10^{-19}, 10^{-20}, 10^{-21}$, and $10^{-22}\,e$ cm respectively. The solid curve corresponds to the experimental bound on the real part of the weak dipole moment of $\tau, 5.6 \times 10^{-18}\,e$ cm. A c.m. energy of 500 GeV and a top-quark mass of 180 GeV are assumed.

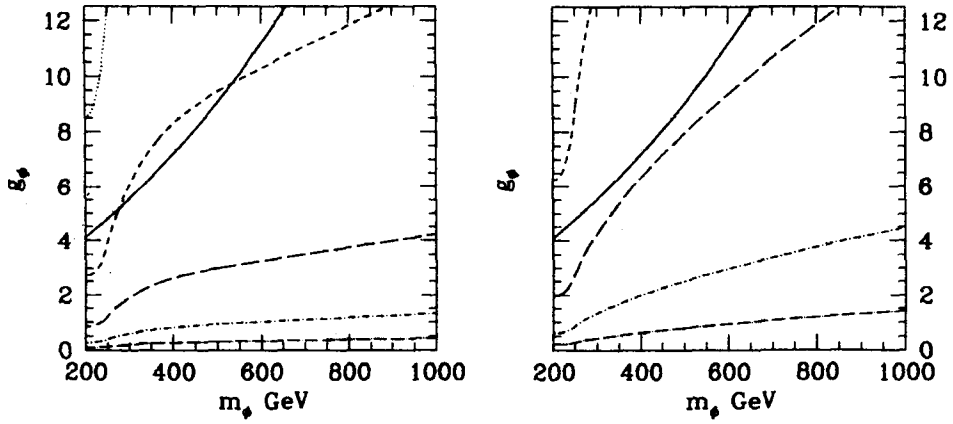

Figure 14. Similar to figure 13 but with contours from the real part of DFFs. The solid lines are the same as in figure 13.

Again, to accommodate constraints on the masses and couplings from Éboli's result we have to have electric dipole form factors of the order of $10^{-22}\,e$ cm or less and weak dipole form factors of the order of $10^{-23}\,e$ cm or less.

5. Conclusions

We have analyzed top and tau electric and weak dipole form factors in models with scalar leptoquarks of weak isopin 0, $\frac{1}{2}$ and 1. We calculate form factors for different values of

$\sqrt{s}$. In general, for leptoquark couplings in the perturbative region and masses allowed by direct experimental searches, large EDFF and WDFF values for both top and tau are possible. In case of the top, the values can be as high as $10^{-20}\,e$ cm, whereas tau form factors can be of the order of $10^{-18}\,e$ cm. The values of form factors are larger for the case of weak isosopin $\frac{1}{2}$, and we have therefore concentrated on that case.

We also obtain contours in the mass-coupling plane corresponding to fixed values of form factors for a given $\sqrt{s}$, and use the experimental limits from LEP on the tau form factors to obtain the allowed region in the plane. This gives constraints on the top form factors. For most of the range of couplings and leptoquark mass, EDFF of the top can be as large as $10^{-19}\,e$ cm, and the WDFF can be as large as $10^{-20}\,e$ cm. We have also used the indirect constraints on the mass and coupling of scalar leptoquarks derived from LEP measurements of the one-loop contribution of leptoquarks to the Z partial decay widths. These constraints are more stringent, and do not permit tau EDFF above about $10^{-19}\,e$ cm and tau WDFF above about $10^{-20}\,e$ cm. The corresponding upper bounds on the top EDFF and WDFF are, respectively, $10^{-22}\,e$ cm and $10^{-23}\,e$ cm.

We thus conclude that though large dipole form factors are allowed in the scalar leptoquark model with parameter values consistent with direct experimental constraints, the indirect constraints from one-loop contributions to Z decay parameters seem to permit only values of form factors which lie below the range likely to be explored in experiments in the foreseeable future.

This, however, does not rule out discovery and observation of other properties of third-generation leptoquarks at linear e^+e^- colliders, if they are not already seen at hadron colliders like Tevatron and LHC. The reason is that the leptoquarks can be pair produced through virtual γ and Z, and would decay with branching ratio of order unity into third generation quark-lepton pair.

It would be interesting to investigate the one-loop contribution of the third-generation leptoquarks to CP violation in the decay $t \to bW$.

Finally, we end with a few comments on comparison of our work with other recent work on DFF in third-generation leptoquark models [6, 7]. Mahanta [6] has estimated the τ EDFF and has reached the conclusion that it can be as high as $10^{-19}\,e$ cm for a choice of g_ϕ and m_ϕ consistent with experimental constraints. He does not discuss the momentum dependence of DFFs. Bernreuther *et al* [7] have obtained the $\sqrt{s}$ dependence of the DFFs of τ. Our results are in agreement with theirs when an overall scale error in their curves is taken into account [24]. Neither [6] nor [7] discuss DFFs of both t and τ in a concerted manner as we have done here.

Acknowledgements

We acknowledge with thanks the initial collaboration of Torsten Arens. We also thank Frank Cuypers for lending his contour-plotting program. One of us (SDR) thanks JWF Valle for his warm hospitality at the University of Valencia where he spent a sabbatical year. This work was supported by DGICYT under grant PB95-1077 and by the TMR network grant ERBFMRXCT960090 of the European Union. SDR was supported by DGICYT sabbatical grant SAB95-0175.

References

[1] ALEPH collab., D Busculic *et al, Phys. Lett.* **B297**, 459 (1992); *Phys. Lett.* **B346**, 371 (1995)
OPAL collab, P D Acton *et al, Phys. Lett.* **B281**, 405 (1992)
OPAL collab., R Ackers *et al, Z. Phys.* **C66**, 31 (1995)
[2] OPAL collab., K Ackerstaff *et al, Z. Phys.* **C74**, 403 (1997)
[3] B Ananthanarayan and S D Rindani, *Phys. Rev.* **D51**, 5996 (1995)
[4] G L Kane, G A Ladinsky and C P Yuan, *Phys. Rev.* **D45**, 124 (1992)
W Bernreuther, O Nachtmann, P Overmann and T Schröder, *Nucl. Phys.* **B388**, 53 (1992); **B406**, 516 (1993) (E)
W Bernreuther, T Schröder and T N Pham, *Phys. Lett.* **B279**, 389 (1992)
D Atwood and A Soni, *Phys. Rev.* **D45**, 2405 (1992)
D Chang, W-Y Keung, and I Phillips, *Nucl. Phys.* **B408**, 286 (1993); **429**, 255 (1994) (E)
W Bernreuther and P Overmann, *Z. Phys.* **C61**, 599 (1994), **C72**, 461 (1996)
B Grzadkowski, *Phys. Lett.* **B305**, 384 (1993)
A Pilaftsis and M Nowakowski, *Int. J. Mod. Phys.* **A9**, 1997 (1994)
F Cuypers and S D Rindani, *Phys. Lett.* **B343**, 333 (1995)
P Poulose and S D Rindani, *Phys. Lett.* **B349**, 379 (1995); *Phys. Lett.* **B383**, 212 (1996); *Phys. Rev.* **D54**, 4326 (1996)
A Bartl, E Christova and W Majerotto, *Nucl. Phys.* **B460**, 235 (1996); **B465**, 365 (1996) (E)
D Atwood and A Soni, BNL-THY-AS-91996, hep-ph/9609418; JLABTH-96-14, hep-ph/9607481
B Grzadkowski and Z Hioki, *Nucl. Phys.* **B484**, 17 (1997); *Phys. Lett.* **B391**, 172 (1997)
[5] C R Schmidt and M E Peskin, *Phys. Rev. Lett.* **69**, 410 (1992)
C R Schmidt, *Phys. Lett.* **B293**, 111 (1992)
J P Ma and A Brandenburg, *Z. Phys.* **C56**, 97 (1992)
A Brandenburg and J P Ma, *Phys. Lett.* **B298**, 211 (1993)
W Bernreuther and A Brandenburg, *Phys. Rev.* **D49**, 4481 (1994)
P Haberl, O Nachtmann and A Wilch, *Phys. Rev.* **D53**, 4875 (1996)
D Atwood, S Bar-Shalom, G Eilam and A Soni, *Phys. Rev.* **D54**, 5412 (1996)
B Grzadkowski and B Lampe, *Phys. Lett.* **B415**, 193 (1997), hep-ph/9706489.
[6] U Mahanta, *Phys. Rev.* **D54**, 3377 (1996)
[7] W Bernreuther, A Brandenburg and P Overmann, *Phys. Lett.* **391**, 413 (1997)
[8] B Adeva *et al, Phys. Lett.* **B261**, 169 (1992)
[9] B Abott *et al, Phys. Rev. Lett.* **81**, 38 (1998), hepex/9803009
[10] F Abe *et al, Phys. Rev. Lett.* **78**, 2906 (1997)
[11] H1 collab., C Adloff *et al, Z. Phys.* **C74**, 191 (1997)
ZEUS collab., J Breitweg *et al, Z. Phys.* **C74**, 207 (1997)
[12] G Altarelli, J Ellis, G F Giudice, S Lola and M L Mangano, *Nucl. Phys.* **B506**, 3 (1997), hep-ph/9703276
M A Doncheski and S Godfrey, *Mod. Phys. Lett.* **A12**, 1719 (1997), hep-ph/9703285
J Blümlein, *Z. Phys.* **C74**, 605 (1997); DESY-97-105, hep-ph/9706362
J Kalinowski, R Ruckl, H Spiesberger and P M Zerwas, *Z. Phys.* **C74**, 595 (1997)
M Suzuki, LBL-40111, hep-ph/9703316.
[13] J Blümlein, E Boos and A Pukhov, *Mod. Phys. Lett.* **A9**, 3007 (1994)
[14] M Hirsch, H V Klapdor-Kleingrothaus and S G Kovalenko, *Phys. Lett.* **B378**, 17 (1996)
U Mahanta, *Phys. Lett.* **B337**, 128 (1994)
S Davidson, D Bailey and B A Campbell, *Z. Phys.* **C61**, 613 (1994)
A A Gvozdev, A V Kuznetsov, N V Mikheev and L A Vasilevskaya, hep-ph/9505229
[15] G Bhattacharyya, J Ellis and K Sridhar, *Phys. Lett.* **B336**, 100 (1994); **338**, 522 (1994) (E).
[16] J K Mizukoshi, O J P Éboli and M C Gonzalez-Garcia, *Nucl. Phys.* **B443**, 20 (1995)
[17] O J P Éboli, IFUSP 1170, hep-ph/9508342
[18] L J Hall and L J Randall, *Nucl. Phys.* **B274**, 157 (1986)
[19] C Q Geng, *Z. Phys.* **C48**, 279 (1990)

[20] W Buchmüller and D Wyler, *Phys. Lett.* **B177**, 377 (1986)
[21] See, for example, M A Doncheski and R W Robinett, *Phys. Lett.* **B411**, 107 (1997), for a discussion.
[22] R E Cutkosky, *J. Math. Phys.* **1**, 429 (1960)
[23] Note that in the case of the top quark, the figures corresponding to imaginary and real parts of EDFF, and real part of WDFF, are plotted in two parts, with different scales for the y axis in the two parts.
[24] W Bernreuther, private communication